Microstructuring of anti-reflection film for HgCdTe/Si IRFPA with femtosecond laser pulse

Shan Zhang (张 姗)[1*], Xiaoning Hu (胡晓宁)[1], Yang Liao (廖 洋)[2], Fei He (何 飞)[2], Changning Liu (刘昌宁)[2], and Ya Cheng (程 亚)[2]

[1]*Key Laboratory of Infrared Imaging Material and Detectors, Shanghai Institute of Technical Physics, Chinese Academy of Sciences, Shanghai 200083, China*

[2]*State Key Laboratory of High Field Laser Physics, Shanghai Institute of Optics and Fine Mechanics, Chinese Academy of Sciences, Shanghai 201800, China*

[*]*Corresponding author: qfzhangshan@163.com*

Received October 26, 2012; accepted November 16, 2012; posted online February 6, 2013

A systematic series of silicon (Si) wafer with microstructured anti-reflection film is prepared by femtosecond laser pulse. The dependence of the morphology and optical properties of the microstructured Si on the experimental parameters is thoroughly investigated. With the laser pulse duration of 40 fs, central wavelength of 800 nm, repetition rate of 250 kHz, laser pulse power of 300 mW, 250 μm/s scanning speed, and 2 μm of displacement between the parallel scans in the air, the quasiordered arrays of grain microstructures on the Si wafer up to 800-nm tall and 800-nm diameter at the bottom offered near-unity transmission in the mid-infrared wavelength. An anti-reflection film of approximately 3 × 3 (mm) is developed on the (211) Si substrate with the optimized parameters, Moreover, up to 30% improvement of the response performance is demonstrated.

OCIS codes: 310.0310, 310.1210, 310.6628, 320.7160.
doi: 10.3788/COL201311.033101.

Third-generation infrared (IR) imaging systems require mercury cadmium telluride (HgCdTe)-based IR focal plane arrays (IRFPAs) of increased formats and multispectral detection capability to meet the advancement in IR technology[1]. HgCdTe photovoltaic detector arrays on a silicon (Si) wafer have been the focus of several studies because of their large wafer size, thermal matching (better reliability) to readout circuitry, and low cost[2,3]. Quantum efficiency is a very important performance parameter of photo-detectors. HgCdTe, as a direct-bandgap semiconductor material, has a large internal quantum efficiency determined by the material quality[4]. Therefore, the quantum efficiency of the detector is mostly determined by the reflected light from the backside illuminated HgCdTe IRFPAs' window. The Si substrate has a large refractive index ($n \approx 3.4$) and reflection loss $R = (\frac{n-1}{n+1})^2$ close to 30% caused by the reflected light from the substrate. Thin film anti-reflection (AR) treatments based on stacks of thin-film materials have been exclusively used to minimize substrate reflections. However, the performance and lifetime of these thin-film AR coatings are limited and can be inadequate for some aerospace and military applications. Radiation exposure and extreme temperature variations can damage the coatings. Several studies have been developing new types of high performance AR treatment for HgCdTe/Si FPAs with wide bandwidth operation, high optical transmission, high durability, and increased lifetime in high radiation environments[5−7]. Femtosecond laser direct-write technique has been comprehensively developed since 1970s[8,9]. However, the AR film made by femtosecond laser for mid-IR (3 –5 μm) FPA has not been investigated. This letter aims to determine the dependence of the amorphous and optical properties of Si microstructure on the laser pulse power and scanning speed, and find an appropriate experimental parameter to realize the near-unity transmission in mid-IR with the AR. The response improvement effect of the AR film on the FPA response was also investigated.

Figure 1 shows a schematic of the experimental setup for femtosecond laser micromachining. A regenerative amplified mode-locked Ti:sapphire laser (Legend USP, Coherent Inc.) with a pulse duration of ∼40 fs, a central wavelength of 800 nm, and a repetition rate of 250 kHz was used to produce the microstructures on the (211) surface of the Si wafer. A circular aperture was used to clip the initial 8.8-mm beam to a 5-mm beam diameter to produce a high quality beam for fabrication. The energy of the fs pulses was adjusted using a neutral density attenuator; the laser beam was focused via a 5× objective lens with a spot size of about 5 μm onto the surface of the substrate, which was mounted on a computer-controlled XYZ stage with a translation resolution of 1 μm. Peng *et al.*[10] indicated that the laser fluence (ϕ) can be written as

$$\phi = (P \cdot t)/S = (P \cdot m)/(f \cdot S), \tag{1}$$

where P is the laser power, t is the interaction time between the laser and the Si, S is the irradiated area of the laser beam, m is the irradiated pulse number, and f is the laser repetition frequency. For the sample affected by moving laser beam, m can be expressed as

$$m = t \times f = \frac{2rt}{v}. \tag{2}$$

ϕ deposited on a single spot can be written as

$$\phi = \frac{2P \times r}{v \times s} = \frac{2P}{\pi v r}, \tag{3}$$

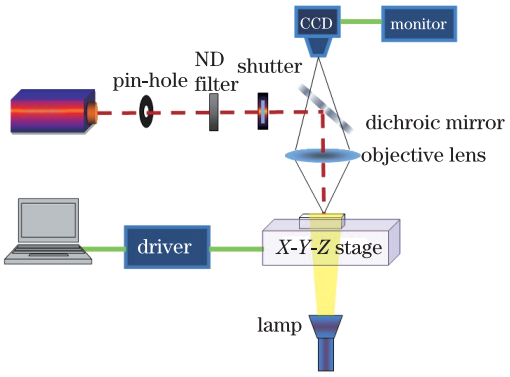

Fig. 1. Schematic of the experimental setup for femtosecond laser micromachining.

where v is the moving velocity of the laser beam and r is the radius of the laser spot. This formation shows that ϕ is proportional to P and v. The morphology of the Si surface was changed using different combinations of P and v.

The reflection of the substrate surface should be minimized and the absorption of the impurities in the microstructures should be avoided to obtain the near-unity IR transmittance[11]. Thus, air was chosen as the ambient gas. Uniform optical quality films with maximum transmittance can be formed by adjusting the experimental conditions, such as pulse energy, translating velocity of the stage, and displacement between the parallel scans. The total transmittance of the films was measured using a Fourier IR spectrograph (NEXUS 670, Nicolet Inc). The morphology and thickness of the films were determined using a scanning electron microscope (SEM).

A (211) Si wafer was cleaned with trichloroethylene, ether, acetone, and methanol, and then dried with a nitrogen gas flow. The sample was then mounted on a three axis translation stage in the air and irradiated in a square area using a femtosecond laser pulse with certain fixed laser energy and translating velocity of 2 μm between the parallel scans. Figure 2 shows the photograph of the Si wafer with a microstructured layer. Figure 3 shows the variations in surface morphology for laser translation velocity, changing from 2 000 to 250 μm/s at a certain laser power of 200 mW. The morphology changed with increasing shot number. At a velocity of 2 000 μm/s, a coarse and honeycombed surface was formed in the microstructured layer. However, the microstructure was inconspicuous. At a velocity of 1 000 μm/s, the surface was coarser and grain structures became distinct. As the velocity continued to decrease to 250 μm/s, the honeycombed surface disappeared and the surface microstructure was sharper and distinct than before. Figure 4 shows the variations in surface morphology for average laser power, changing from 125 to 300 mW at the moving velocity of 250 μm/s. Both the microstructure height and distance between the microstructures increased when the laser power was less than 200 mW. When the laser power was larger than 200 mW, the changes in morphology was small and the surface of the sample showed some small debris. The formation of the debris may be related to the gas atmosphere and experimental condition which resulted in comparatively large liquid state associated with the slow evaporation of atomic gas from the molten material prior to solidification[12].

The cross-sectional profile of the structure in the AR surface texture has a significant impact on the AR performance. Figure 5 shows the measured transmittance for the unstructured and microstructured Si, as well as the theoretical value for one surface of Si. The transmittance of the surface with distinct microstructure improved drastically over the mid-IR spectrum. The highest performance over the widest bandwidth was 70% by the AR-textured Si wafer. For a single-side textured Si wafer, the reflection on the other side of the wafer was 30%. Therefore, the transmittance of the AR textured side was near 100%. The degree of improvement was proportional to the distinctness of the conical structures. A big absorption loss

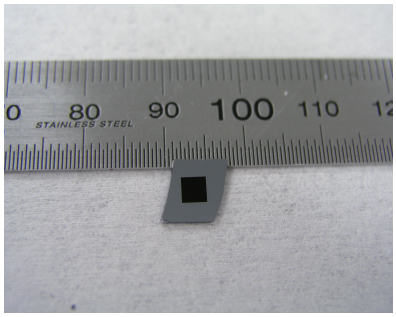

Fig. 2. Photograph of Si sample treated by femtosecond laser.

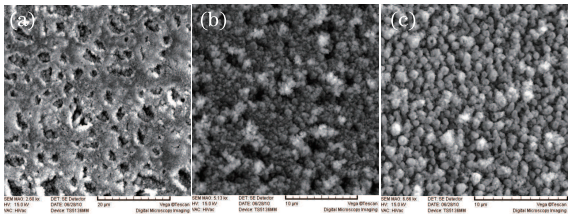

Fig. 3. SEMs of a (211) Si surface after irradiation with a laser translation velocity of (a) 2 000, (b) 1 000, and (c) 250 μm/s. Each SEM is taken normal to the surface.

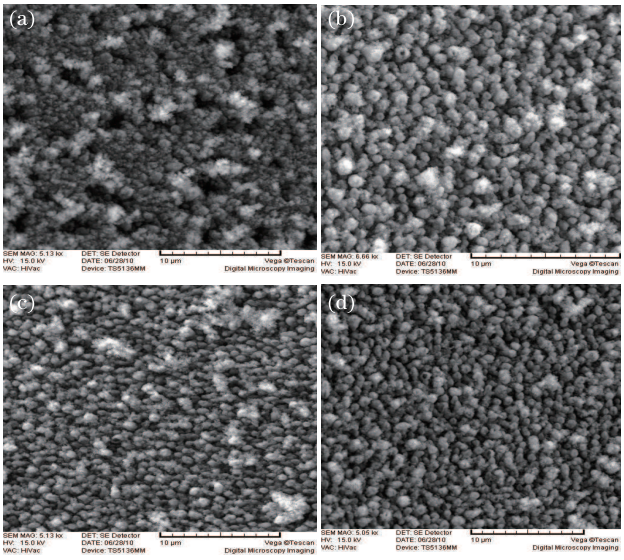

Fig. 4. SEMs of a (211) Si surface after irradiation with laser power of (a) 125, (b) 200, (c) 250, and (d) 300 mW. Each SEM is taken normal to the surface.

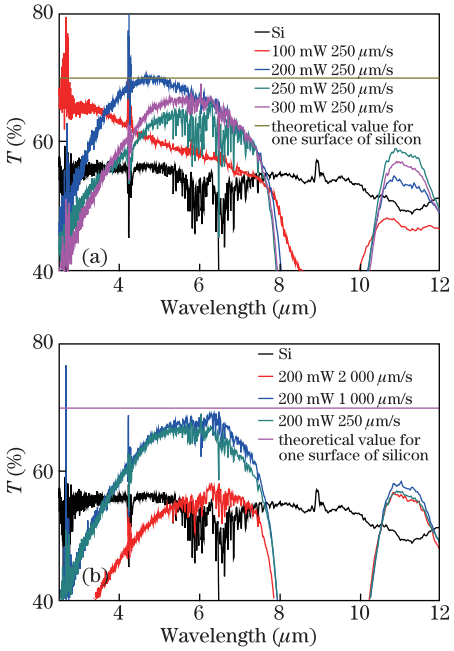

Fig. 5. (Color online) Transmittance of microstructured Si for different conditions. Wavelength dependence of the transmittance (a) on the translation velocity of laser pulse and (b) on the average power of laser pulses used in microstructuring. For reference, the same measurements are shown for unstructured (211) Si.

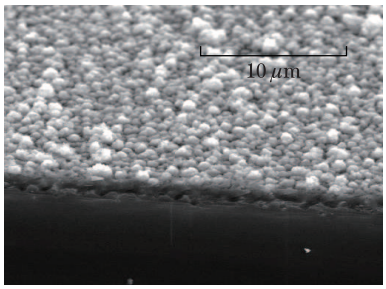

Fig. 6. SEM of a (211) Si surface after irradiation with laser power.

was observed over a wavelength range spanning 8 to 11 μm. The origin of the big absorption may be attributed to the incorporation of a high density of oxygen impurity that originated from the atmosphere or the Si material itself[13].

The 40-fs duration, central wavelength of 800 nm, repetition rate of 250 kHz, laser pulse of 300 mW power, 250 μm/s of scanning speed, and 2 μm of displacement between the parallel scans in the air are the best experiment parameters to the distinct microstructure and near-unity transmittance. The Si wafer contain quasiordered arrays of grain microstructures up to 800-nm tall and 800-nm diameter at the bottom, as shown in Fig. 6.

A square area of approximately 3 × 3 (mm) was obtained by femtosecond laser irradiation on the Si substrate of HgCdTe/Si FPA using the optimized experiment parameters. The sample photograph is shown in Fig. 7. The detector (HgCdTe/Si) size was 10 × 8 (mm), and can respond to spectrum smaller than 5 μm. The HgCdTe/Si detector was hybridized to Si readout integrated circuit using in column and applied to the fanout. The performance of the 320 × 256 elements mid-IR wavelength HgCdTe/Si FPA with the new AR film was tested after encapsulation in dewar and measured at $f/2.7$ with a frame bias of 1 100 mV and an integration time of 2 000 μs in 77 K. The AR-textured area was darker than the untreated area because of the reflect alleviation by the micromachining structures. Through the FPA performance tested system, the photocurrent of the pixel can be tested and calculated to the response. At the tested condition, the response map of the FPA is shown in Fig. 8. The degree of grey exhibits the magnitude of the response; the darker color corresponds to the larger response. The microtextured area showed increasing response than that of the untreated area. Figure 6 shows the response histogram of the pixel along the direction vertical to each other. The laser structured area (1.25×10^8 A/W) and untreated area (0.95×10^8 A/W) exhibited 30% elevation of pixel response. For the photovoltaic IR detector, the relationship between the response and quantum was $R = \lambda\eta/hc$, where R is the response, η is the quantum, λ is the cutoff wavelength of the diode, h is the plank constant, and c is the speed of light. In this study, λ=0.5 μm, $h \equiv 6.626 \times 10^{-34}$ J·s, and $c \equiv 3 \times 10^8$ m/s. Thus, the increases of response corresponded to the improvement of the detector quantum efficiency.

In conclusion, the (211) surface of a Si wafer is microstructured by 250-kHz femtosecond laser in the air. Various parameters, such as spot size, energy density, number of shots, and scanning parameter, are used to make appropriate microstructure topography. The impurity and structural defects into the lattice in the microstructuring process can be avoided with the appropriate ambient gas. The microstructure arrays provided a gradual change of the refractive index for light

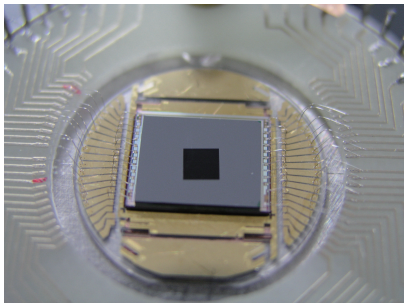

Fig. 7. Photograph of FPA with the new anti-reflection film.

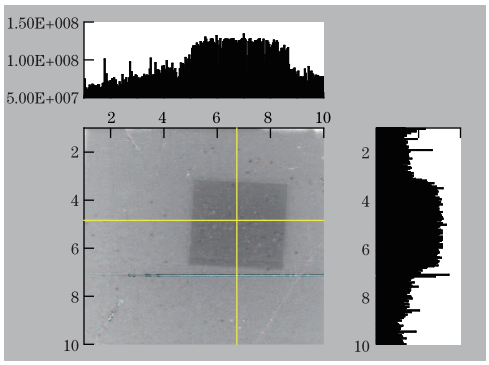

Fig. 8. Response performances of FPA with the new anti-reflection film.

propagating from air into the Si. The transmission is reduced to a minimum for the mid-IR region. The femtosecond laser micromachining has low effect on the HgCdTe performance with high precision, low heat effect, and damage threshold. Using the optimal experiment parameters, FPA with AR by femtosecond laser microstructuring in the substrate is developed and tested. The FPA with the new AR film has higher quantum efficiency than that of the untreated substrate.

This work was supported by the Opening foundation of Key Laboratory of Infrared Imaging Material and Detectors, Shanghai Institute of Technical Physics, CAS.

References

1. A. Rogalski, J. Antoszewski, and L. Faraone, J. Appl. Phys. **105,** 091101 (2009)
2. S. M. Johnson, W. A. Radford, A. A. Buell, M. F. Vilela, J. M. Peterson, J. J. Franklin, R. E. Bornfreund, A. C. Childs, G. M. Venzor, M. D. Newton, E. P. G. Smith, L. M. Ruzicka, G. K. Pierce, D. D. Lofgreen, T. J. de Lyon, and J. E. Jensen, Proc. SPIE **5732,** 250 (2005).
3. N. K. Dhar and M. Z. Tidrow, Proc. SPIE **5564,** 34 (2004).
4. R. K. Willardson and A. C. Beer, *Semiconductors and Semimetals* (Academic, New York, 1981).
5. D. S. Hobbs and B. D. MacLeod, Proc. SPIE **6720,** 67200L (2007).
6. B. D. MacLeod and D. S. Hobbs, Proc. SPIE **6940,** 69400Y (2008).
7. J. Zhao, A. Wang, and M. A. Green, Appl. Phys. Lett. **73,** 1991 (1998).
8. Y. Lin, M. H. Hong, T. C. Chong, C. S. Lim, G. X. Chen, L. S. Tan, Z. B. Wang, and L. P. Shi, Appl. Phys. Lett. **89,** 041108 (2006).
9. M. L. Tseng, Y. W. Huang, M. K. Hsiao, H. W. Huang, H. M. Chen, Y. L. Chen, C. H. Chu, N. N. Chu, Y. J. He, C. M. Chang, W. C. Lin, D. W. Huang, H. P. Chiang, R. S. Liu, G. Sun, and D. P. Tsai, ACS Nano **6,** 5190 (2012).
10. Y. Peng, Y. Wen, D. Zhang, S. Luo, L. Chen, and Y. Zhu, Appl. Opt. **50,** 4765 (2011).
11. C. H. Crouch, J. E. Carey, M. Shen, E. Mazur, and F. Y. Genin, Appl. Phys. A **79,** 1635 (2004) .
12. T. Matsumura, A. Kazama, and T. Yagi, Appl. Phys. A **81,** 1393 (2005).
13. Y. Liu, "The optical properties of the microstructured silicon made by femtosecond laser (in Chinese)", Master Thesis (Fudan University, 2007).